OFFICE OF NAVAL RESEARCH

GRANT N00014-94-1-0540

R & T Code 3132111

Kenneth J. Wynne

Technical Report No. 6

Effects of Molecular Structure on the Electroactive and Optical Properties of Conjugated
Rigid-Rod Polybenzobisazoles

by

John A. Osaheni and Samson A. Jenekhe

Prepared for Publication

in

Chemistry of Materials

University of Rochester
Department of Chemical Engineering
Rochester, NY

March 20, 1995

Accesion For		
NTIS CRA&I	☑	
DTIC TAB	☐	
Unannounced	☐	
Justification		
By		
Distribution /		
Availability Codes		
Dist	Avail and / or Special	
A-1		

19950403 019

REPORT DOCUMENTATION PAGE

Public reporting burden for this collection of information is estimated to average 1 hour per response, including the time for reviewing instructions, searching existing data sources, gathering and maintaining the data needed, and completing and reviewing the collection of information. Send comments regarding this burden estimate or any other aspect of this collection of information, including suggestions for reducing this burden, to Washington Headquarters Services, Directorate for Information Operations and Reports, 1215 Jefferson Davis Highway, Suite 1204, Arlington, VA 22202-4302, and to the Office of Management and Budget, Paperwork Reduction Project (0704-0188), Washington, DC 20503.

1. AGENCY USE ONLY (Leave blank)	2. REPORT DATE	3. REPORT TYPE AND DATES COVERED
	March 20, 1995	Technical Report # 6

4. TITLE AND SUBTITLE

Effects of Molecular Structure on the Electroactive and Optical Properties of Conjugated Rigid-Rod Polybenzobis-azoles.

5. FUNDING NUMBERS

N00014-94-1-0540

6. AUTHOR(S)

J. A. Osaheni and S. A. Jenekhe

Kenneth J. Wynne
R & T Code: 3132111

7. PERFORMING ORGANIZATION NAME(S) AND ADDRESS(ES)

Department of Chemical Engineering
University of Rochester
206 Gavett Hall
Rochester, NY 14627-0166

8. PERFORMING ORGANIZATION REPORT NUMBER

6

9. SPONSORING/MONITORING AGENCY NAME(S) AND ADDRESS(ES)

Office of Naval Research
800 North Quincy Street
Arlington, VA 22217-5000

10. SPONSORING/MONITORING AGENCY REPORT NUMBER

DTIC
ELECTE
APR 0 4 1994
F

11. SUPPLEMENTARY NOTES

Accepted for publication in *Chemistry of Materials*.

12a. DISTRIBUTION/AVAILABILITY STATEMENT

Reproduction in whole in in part is permitted for any purpose of the United States Government.
This document has been approved for public release and sale; its distribution is unlimited.

12b. DISTRIBUTION CODE

13. ABSTRACT (Maximum 200 words)

The effects of molecular structure on the electronic structure and electrochemical and linear optical properties of a series of π-conjugated rigid-rod polybenzobisazoles, including three new polymers, were explored by cyclic voltammetry and measurement of the optical dispersion of the refractive index. The electrochemical reduction of the polymers was reversible whereas oxidation was not reversible in accord with the electron deficient nature of the *benzobisazole* ring. The observed variation of the reduction and oxidation potentials, electron affinity, and ionization potential of the series of polymers was related to the variation in backbone structure. The electron affinity of the polymers was 2.4 to 3.0 eV which indicated that the LUMO energy level was tunable by up to 0.6 eV. The ionization potential (5.2 to 5.7 eV) and associated HOMO level of the polymers was tunable by up to 0.5 eV. The measured wavelength dispersion of the refractive index of the polybenzobisazoles showed that $n(\lambda = 1064 \text{ nm})$ and $n(\lambda = 2500 \text{ nm})$ were 1.74-2.03 and 1.55-1.95 respectively. The large refractive index variation with molecular structure was satisfactorily accounted for by the competing effects of polarizability and molar volume. These results provide a basis for understanding the electronic, optoelectronic, and optical properties of the conjugated polybenzobisazoles in terms of the underlying molecular and electronic structures.

14. SUBJECT TERMS

Conjugated polymers; polybenzobisazoles; electroactive polymers; effects of structure; refractive index dispersion.

15. NUMBER OF PAGES
52

16. PRICE CODE

17. SECURITY CLASSIFICATION OF REPORT	18. SECURITY CLASSIFICATION OF THIS PAGE	19. SECURITY CLASSIFICATION OF ABSTRACT	20. LIMITATION OF ABSTRACT
Unclassified	Unclassified	Unclassified	Unlimited

TECHNICAL REPORT DISTRIBUTION LIST - GENERAL

Office of Naval Research (1)*
Chemistry and Physics Division
Ballston Tower 1, Room 503
800 North Quincy Street
Arlington, Virginia 22217-5660

Defense Technical Information
  Center (2)
Building 5, Cameron Station
Alexandria, VA 22314

Dr. James S. Murday (1)
Chemistry Division, Code 6100
Naval Research Laboratory
Washington, D.C. 20375-5000

Dr. Kelvin Higa (1)
Chemistry Division, Code 385
Naval Air Weapons Center
  Weapons Division
China Lake, CA 93555-6001

Dr. Peter Seligman (1)
Naval Command, Control and
  Ocean Surveillance Center
RDT&E Division
San Diego, CA 92152-5000

Dr. Richard W. Drisko (1)
Naval Civil Engineering
  Laboratory
Code L52
Port Hueneme, CA 93043

Dr. Harold H. Singerman (1)
Naval Surface Warfare Center
  Carderock Division Detachment
Annapolis, MD 21402-1198

Dr. Eugene C. Fischer (1)
Code 2840
Naval Surface Warfare Center
  Carderock Division Detachment
Annapolis, MD 21402-1198

* Number of copies to forward

Effects of Molecular Structure on the Electroactive and Optical Properties of Conjugated Rigid-Rod Polybenzobisazoles

John A. Osaheni[†] and Samson A. Jenekhe[*]

Department of Chemical Engineering and Center for Photoinduced Charge Transfer,

University of Rochester, Rochester, New York 14627-0166.

ABSTRACT

The effects of molecular structure on the electronic structure and electrochemical and linear optical properties of a series of π-conjugated rigid-rod polybenzobisazoles, including three new polymers, were explored by cyclic voltammetry and measurement of the optical dispersion of the refractive index. The electrochemical reduction of the polymers was reversible whereas oxidation was not reversible in accord with the electron defficient nature of the *benzobisazole* ring. The observed variation of the reduction and oxidation potentials, electron affinity, and ionization potential of the series of polymers was related to the variation in backbone structure. The electron affinity of the polymers was 2.4 to 3.0 eV which indicated that the LUMO energy level was tunable by up to 0.6 eV. The ionization potential (5.2 to 5.7 eV) and associated HOMO level of the polymers was tunable by up to 0.5 eV. The measured wavelength dispersion of the refractive index of the polybenzobisazoles showed that $n(\lambda = 1064 \text{ nm})$ and $n(\lambda = 2500 \text{ nm})$ were 1.74-2.03 and 1.55-1.95, respectively. The large refractive index variation with molecular structure was satisfactorily accounted for by the competing effects of polarizability and molar volume. These results provide a basis for understanding the electronic, optoelectronic, and optical properties of the conjugated polybenzobisazoles in terms of the underlying molecular and electronic structures.

† Current Address: General Electric Corporate Research & Development, P. O. Box 8, CEB412, Schenectady, NY 12301.

* To whom correspondence should be addressed.

INTRODUCTION

The promise of π-conjugated polymers as advanced materials[1-6] for applications in electronics, optoelectronics, and nonlinear optics has motivated our continuing investigation of several classes of π-conjugated polymers.[7-22] These studies have included synthesis and characterization of new conjugated polymers and copolymers[7-10], thin film processing[11-12], investigation of photophysical properties (e.g. photoconductivity[13-15], third-order optical nonlinearity[16-20], and luminescence[7b,21,22]) and exploration of device applications. For example, xerographic photoreceptors made from π-conjugated polybenzobisazoles have good photosensitivity and high quantum efficiency for charge photogeneration.[15] In the areas of photonic and nonlinear optical applications, waveguiding with p-conjugated polymers requires materials which can be processed into high optical quality films with low linear optical losses and relatively high refractive index which assures good field confinement.[6] Initial efforts in the fabrication of waveguide devices from poly(p-phenylene benzobisthiazole) and poly(2,2'-(1,4-phenylene)-6,6'-bis(4-phenylquinoline)) have also been successful.[23] In order to better understand as well as to optimize the materials for these applications, the effects of molecular structure and morphology on the electronic structure and solid state properties need to be elucidated. In particular, knowledge of the effects of molecular structure on the electrochemical properties and associated electronic structure (electron affinity and ionization potential) is needed for understanding not only the well-known ground-state charge transfer complexes (i.e. doped conducting polymers)[1,22] but also the recently discovered *excited-state charge transfer complexes*[21,22] of conjugated polymers. Although the refractive index of conjugated polymers is one of the fundamental properties of interest in their applications in optoelectronic and photonic devices[3,4,6,23], there has been very few reports of its

measurement until the recent detailed investigation of the structure-refractive index relationships in conjugated polyimines.[24] This is in contrast to the large experimental data base of refractive indices of *nonconjugated* polymers[25] and an accurate group contribution method for their computational prediction.[26]

One class of π-conjugated polymers that has attracted significant efforts in our laboratory[7,18,19] and other laboratories[27-29] is the heterocyclic rigid-rod polybenzobisazole family which includes polybenzobisthiazoles, polybenzobisoxazoles and polybenzobisimidazoles. This class of polymers exhibits high tensile strength, high modulus, and excellent thermal and environmental stability.[27-29] The high strength of these materials arises from the ability to achieve a high degree of molecular order during fiber or film processing. The solutions of these polymers in strong acids or in Lewis acid/nitromethane[12,30] can exist in either optically isotropic or anisotropic liquid crystalline phases, depending on the concentration, molecular weight or temperature. Recently[7a], we showed that a systematic incorporation of *trans*-polyene moieties in place of the the *p*-phenylene ring in poly(*p*-phenylene benzobisthiazole) (PBZT) leads to a wide variation of the electronic absorption spectra, thus providing model polymers for probing structure-property relationships in this class of materials. We have also shown that the polybenzobisazoles are promising nonlinear optical materials as demonstrated by the large third-order nonlinear optical susceptibility of PBZT[18] and poly(*p*-phenylene benzobisoxazole) (PBO).[19] More recently we have found that the polybenzobisazoles have interesting light emitting properties[7b,21,22,31] and good photoconductivity.[15,22] Although many conjugated polybenzobisazoles have been synthesized and aspects of their photoactive and electronic properties investigated, a systematic study of the evolution of

their electronic structure and electroactive and photoactive properties with molecular structure has not been done experimentally or theoretically. Our present study aims to explore the relationship of polymer molecular structure with electroactive and photoactive properties of the polybenzobisazoles.

In this paper, we report investigation of the electrochemical properties of a series of 8 conjugated polybenzobisazoles whose molecular structures are shown in Chart **I**. Three of these polymers are new and were synthesized and characterized for this study: poly(4,4'-biphenylene benzobisthiazole) (PBBZT, **1a**), poly(2,6-naphthalene benzobisthiazole) (2,6-PNBT, **1b**), and poly(1,4-naphthalene benzobisthiazole) (1,4-PNBT, **1c**). The synthesis and characterization of the remaining 5 polymers in Chart **I** have been reported.[7,27] The isotropic refractive index of the new polymers as well as those of PBZT (**1d**), poly(benzobisthiazole-1,4-phenylenebisvinylene) (PBTPV, **1e**), poly(benzobisthiazole vinylene) (PBTV, **1f**), poly(benzobisthiazole divinylene) (PBTDV, **1g**), PBO (**2**), and four polybenzobisimidazoles (Chart **II**) was also investigated. The diverse molecular structures investigated in this study provide a systematic approach for understanding the structure-property relationships in the electroactive and photoactive properties of the polybenzobisazoles.

EXPERIMENTAL SECTION

Materials and purification. 2,5-Diamino-1,4-benzenedithiol dihydrochloride (DABDT) was obtained from Daychem (Dayton, OH) and was purified by recrystallization under nitrogen atmosphere using the literature method[28a]. 4,4'-Biphenyldicarboxylic acid (97%, Aldrich), 1,4-naphathalenedicarboxylic acid (Aldrich), and 2,6-naphthalenedicarboxylic acid (>98%, Lancaster) were also recrystallized prior to use.

Polyphosphoric acid (PPA) and 85% phosphoric acid were purchased from Aldrich Chemical and were used as received to prepare 77% polyphosphoric acid used in the dehydrochlorination of DABDT and subsequently as the polymerization medium. Phosphorous pentoxide (P_2O_5) was obtained from Baker Inc.

Poly(4,4'-biphenylene benzobisthiazole) (PBBZT). 1.3 g (5.3 mmol) of 2,5-diamino-1,4-benzenedithiol dihydrochloride (DABDT) was dissolved in 13.7 g of 77% PPA (dearated). Dehydrochlorination of DABDT was carried out at 70 ^oC under vacuum. After complete dehydrochlorination, the reaction vessel was cooled to 50 ^oC, and 1.28 g (5.3 mmol) of 4,4'-biphenyldicarboxylic acid was added under nitrogen purge together with 6.7 g of fresh P_2O_5. The reaction mixture was stirred slowly and the temperature raised to 100 ^oC (4 h), then to 140 ^oC (8 h) and finally held at 180 ^oC for 24 h. The polymerization dope was cooled down to room temperature and precipitated in water. The polymer was shredded into small pieces with a blender to facilitate purification which consisted of extraction for 2 days with a large volume of water followed by drying in a vacuum oven at 80 ^oC for 12 hours. $[\eta]$ = 5.5 dL/g (30 ^oC in methanesulfonic acid); ^{1}H NMR ($CD_3NO_2/AlCl_3$, ppm): δ = 8.3 (m, 4H), 8.5 (m, 4H), 9.2 (s, 2H). FTIR (free standing film, cm^{-1}): 3068, 3022, 1605, 1554, 1515, 1481, 1426, 1402, 1313, 1249, 1208, 1182, 1130, 1115, 1057, 1003, 960, 860, 820, 700, 603.

Poly(2,6-naphthalene benzobisthiazole) (2,6-PNBT). 1.0 g (4.08 mmol) of DABDT was dissolved in 9.8 g of 77% PPA (dearated) and dehydrochlorination was carried out at 70 ^oC under vacuum. After complete dehydrochlorination, the reaction vessel was cooled to 50 ^oC, and 0.88 g (4.08 mmol) of 2,6-naphthalenedicarboxylic acid was

added under nitrogen purge together with 5 g of fresh P_2O_5. The reaction mixture was stirred slowly and a temperature profile identical to that used in PBBZT synthesis was employed. The polymerization dope was cooled down to room temperature and precipitated in water. Purification was carried out in a similar fashion to that of PBBZT. $[\eta] = 7.3$ dL/g (30 °C in methanesulfonic acid); ^{1}H NMR (CD_3NO_2/AlCl$_3$, ppm): $\delta = 8.2$ (m, 2H), 8.5 (m, 4H), 9.3 (s, 2H). FTIR (free standing film, cm^{-1}): 3075-3033, 1625, 1603, 1506, 1429, 1404, 1382, 1337, 1309, 1277, 1250, 1210, 1192, 1170, 1055, 984, 960, 882, 860, 811, 690, 677.

Poly(1,4-naphthalene benzobisthiazole) (1,4-PNBT). 1.0 g (4.08 mmol) of DABDT was dissolved in 9.8 g of 77% PPA (dearated) and dehydrochlorination was carried out at 70 °C under vacuum. After complete dehydrochlorination, the reaction vessel was cooled to 50 °C, and 0.88 g (4.08 mmol) of 1,4-naphthalenedicarboxylic acid was added under nitrogen purge together with 5 g of fresh P_2O_5. The polymerization temperature profile and subsequent isolation and purification steps were identical to those of 2,6-PNBT. $[\eta] = 5.0$ dL/g (30 °C in methanesulfonic acid); ^{1}H NMR (CD_3NO_2/AlCl$_3$, ppm): $\delta = 8.1$ (m, 2H), 8.6 (m, 4H), 9.4 (s, 2H). FTIR (free standing film, cm^{-1}): 3075-3033, 1610, 1507, 1515, 1426, 1404, 1382, 1315, 1249, 1208, 1182, 1089, 1055, 1003, 926, 854, 835, 761, 695, 684.

Preparation of thin films

Films for optical absorption spectra, FTIR spectra, and refractive index measurements were prepared by using the complexation-mediated solubilization approach.[12] Dilute solutions of the polymers, <0.5wt% polymer in AlCl$_3$ or

GaCl$_3$/nitromethane solution were used to prepare thin films on fused silica substrates for optical absorption measurements. In order to obtain thicker films on fused silica substrates or free standing films for FTIR, solutions of varying concentrations (1-3wt%, depending on the molecular weight of the polymer) were prepared with the Lewis acid in slight excess of the stoichiometric requirement to facilitate spin coating in ambient conditions. The polymer solutions were isotropic since the concentrations employed were well below the critical concentration at which the rigid-rod polymers exhibit liquid crystallinity (5-10 wt%).[12,30] The films of the polymer-Lewis acid complex were washed with deionized water, and subsequently placed in a beaker of fresh deionized water to be decomplexed overnight. The films were dried at 80 °C in a vacuum oven for 6-8 h. The film thickness was measured with Alpha Step profilometer (Tencor Instruments) which has a resolution of 1 nm. The film thickness was in the range of 20-80 nm for samples used to obtain optical absorption spectra whereas 1 to 2.5 µm thick films were used for the refractive index measurements.

Characterization.

Intrinsic viscosity [η] of the polymers was measured in methanesulfonic acid at 30 °C using a Cannon Ubbelohde capillary viscometer. Thermogravimetric analysis (TGA) and differential scanning calorimetry (DSC) were done using a Du Pont Model 2100 Thermal Analyst based on an IBM PS/2 Model 60 computer and equipped with a Model 951 TGA and a Model 910 DSC units. The TGA data were obtained in flowing nitrogen at a heating rate of 10 °C/min whereas the DSC thermograms were obtained in nitrogen at a heating rate of 20 °C/min. FTIR spectra were taken at room temperature using a Nicolet Model 20SXC Fourier transform infrared (FTIR) spectrometer under nitrogen purge. The ^{1}H NMR

spectra were taken at 300 MHz using a General Electric Model QE 300 instrument. Polymer solutions for NMR spectra were prepared in a dry box, using deuterated nitromethane (CD_3NO_2) containing aluminum (III) chloride.

Optical absorption spectra of thin films and solutions of the polymers were obtained with a Perkin Elmer Model Lamda 9 UV-Vis-near IR spectrophotometer in the wavelength range 190-3200 nm. The optical transmission spectra of thick films (1.0 - 2.5 μm) were obtained and the resulting interference fringes of the films, i. e. the consecutive wavelengths at which the maxima and minima transmission occurred were used to deduce the refractive index. The data were obtained in the range 700-2800 nm, with the probe beam perpendicular to the plane of the films. The slit of the spectrophotometer was set at 1nm. The refractive index was calculated using the approach described by swanepoel.[32] The detailed analysis and data regression for the determination of refractive index of conjugated polymers have been described previously.[24]

Cyclic voltammograms of thin films of the polymers were done by using EG&G Princeton Applied Research potentiostat/galvanostat Model 270 equipped with Electrochemical Analysis System software based on IBM PS/2 Model 60 computer. The experimental setup was in the single cell and three-electrode configuration. Platinum wires were used as both the counter and working electrodes, and Ag/Ag^+ (silver wire in 0.1M $AgNO_3$ in the electrolyte solution) was used as a reference electrode. The Ag/Ag^+ was calibrated with ferrocene as the internal standard. Thin films of the polymers on platinum electrodes were prepared by dipping the electrode into a 0.2-1.0 wt% polymer solution and the resulting film rigorously washed with water and dried in a vacuum oven at 80 °C. A 0.1M tetrabutylammonium tetrafluoroborate (TBABF) (Aldrich) in ultra pure acetonitrile

(99+%, Johnson Matthey Electronics) was used as the electrolyte. The potential values were referenced back to the saturated calomel electrode (SCE) potential by using the ferrocene/ferrocenium couple as the internal standard. The reported cyclic voltammograms were obtained at voltage scanning rate of 20 mV/s.

RESULTS AND DISCUSSION

New Polymers: Molecular Structure and Optical Absorption Spectra

The molecular structures of the new polymers, PBBZT, 2,6-PNBT, and 1,4-PNBT, were established by both ^{1}H NMR and FTIR spectra. Figure 1 shows the ^{1}H NMR spectrum of PBBZT obtained in nitromethane containing aluminum trichloride. The number of protons corresponding to each resonance is in agreement with the proposed structure. Figure 2 shows the ^{1}H NMR spectrum of 1,4-PNBT and its assignment. As expected, there are three main resonances and the number of protons corresponding to each resonance is in good agreement with the proposed structure. The ^{1}H NMR spectrum of 2,6-PNBT was also found to be in good agreement with the proposed structure.

Figure 3 shows a comparison of the FTIR spectra of PBBZT, 2,6-PNBT, and 1,4-PNBT along with that of PBZT. The characteristic bands of the polybenzobisthiazoles can be observed in the three new polymers. The FTIR spectrum of PBBZT shows essentially identical bands as that of PBZT except for the new band at 1003 cm^{-1} in PBBZT, and the slight differences in the relative intensities of the other bands. In PBZT, the heteroring stretch associated with the thiazole ring shows intense bands at 1485 and 1314 cm^{-1} while the heteroring breathing and out-of-plane ring deformation are at 960 and 689 cm^{-1}, respectively.[7,33] The frequency of the heteroring stretches at 1485 cm^{-1} in PBZT is shifted in 2,6-PNBT and 1,4-PNBT to ~1507 cm^{-1}. The heteroring breathing bands appear at 882

and 926 cm^{-1} respectively, in 2,6-PNBT and 1,4-PNBT. This represent a decrease in frequency (or increase in the force constant of this motion) by 78 and 34 cm^{-1} respectively relative to those of PBZT. The features of the FTIR spectra of 2,6- and 1,4-PNBT while similar, show a number of differences especially in the out-of-plane C-H stretching region (860-750 cm^{-1}) which reflects the substitution pattern of the naphthalene ring. Overall, the FTIR spectra are consistent with the proposed structures of the new polymers.

The intrinsic viscosities of PBBZT, 2,6-PNBT, and 1,4-PNBT were 5.5, 7.3, and 5.0 dL/g, respectively, indicating modest molecular weights of ~15,000-17,700, using the known Mark-Houwink relationship for PBZT.[28a] Each of these polymers was readily processed into thin films on substrates or as free standing films for various analysis. The TGA thermograms of PBBZT and 2,6-PNBT obtained in flowing nitrogen at 10 ^{o}C/min are shown in Figure 4. The thermal stability of the new polymers is quite high, starting to decompose at ~700 ^{o}C in nitrogen atmosphere, and similar to PBZT (720 ^{o}C).[7] The DSC thermograms of the new polymers did not show any thermal transition (such as T_g or T_m) below the decomposition temperature similar to what is observed in PBZT. Thus, the new aromatic-linked polybenzobisthiazoles are, as expected, also high temperature materials.

Figure 5 shows the optical absorption spectra of thin films of PBBZT, 2,6-PNBT, 1,4-PNBT along with that of PBZT. A summary of the optical properties, including the λ_{max} and the optical absorption edge (E_g^{opt}), of the new polymers as well as those shown in Chart **I** is given in Table 1. The 2,6-PNBT and PBZT show similar absorption features (λ_{max} and E_g^{opt} are identical), whereas the optical absorption spectra of PBBZT and 1,4-PNBT are different from those of PBZT. The absorption spectrum of PBBZT is blue shifted from that of PBZT's absorption edge (E_g^{opt}) by 0.13 eV. On the other hand, the π-π^{*} absorption threshold of 1,4-PNBT (2.36 eV) is red shifted relative to that of PBZT. The

absorption spectrum of 1,4-PNBT shows broad features unlike the well resolved vibronic structures in the spectra of 2,6-PNBT and PBZT. This implies that the 1,4- subsitution pattern of the naphthalene ring introduces significant disorder to the polymer. Figure 6 shows the solution optical absorption spectra of the new polymers in methanesulfonic acid. The trend of the optical absorption spectra in solution is quite different from that of the solid state. The absorption threshold is identical in all the polymers whereas the λ_{max} is at 440, 444, and 465 nm respectively, for 1,4-PNBT, PBBZT, and 2,6-PNBT. The results of the solution spectra imply that the planarity of the polymer repeat units is similar when they are protonated, whereas in the solid state the geometry is different for the three polymers. In addition, the difference in spectral features, e.g. lineshape, between the dilute solution (Figure 6) and the thin film (Figure 5) optical spectra of the same polymer can similarly be explained by the effects of protonation in solution and strong intermolecular interactions between chains in the solid state.

Electrochemical Properties and Electronic Structure

The effects of molecular structure on the electroactive properties and electronic structure of the polybenzobisazoles shown in Chart I were explored through measurement of the electrochemical reduction and oxidation (redox) properties. To facilitate the discussion of the results, we use the 1,4-phenylene-linked polymer (PBZT) as a reference and compare the redox properties of the other polybenzobisazoles to that of PBZT. It has been shown from similar studies of the redox properties of the rigid-rod polyquinolines that side group substitution of electron withdrawing or donating groups had negligible effect on the electronic structure of the polymers compared with changes in the backbone

structure.[34] Here we explore the effects of different moieties introduced into the backbone as well as the heteroatom of the polybenzobisazoles (Chart I). The heterocyclic *benzobisthiazole* and *benzobisoxazole* rings are electron defficient groups so that one might expect the polymers in Chart I to be more susceptible to reduction (electron accepting) than oxidation. It is interesting to see to what extent the different **R**-moieties and heteroatoms (S or O) regulate or modify the redox properties and electronic structure.

Electrochemical Reduction. Figure 7 shows the cyclic voltammograms (CVs) of the reduction of PBZT and that of 2,6-PNBT. It is observed that both polymers exhibit reversibility with identical onset of the reduction (E^{red}_{onset} = -1.75 V vs. SCE). However, the cathodic peak (E_{pc}) and anodic peak (E_{pa}) potentials are shifted away from each other with the difference in peak potentials ($\Delta E_p = E_{pa}-E_{pc}$) being larger in 2,6-PNBT (0.53 V) compared to that of PBZT (0.34 V). These ΔE_p values are quite large and typical of many π-conjugated polymers in the solid state.[35,36] The origin of the large peak separation may be due to redox-related structural reorganization within the films which affect diffusion of counterions in and out of the polymers. The morphology of the polymer film is another factor that may affect ΔE_p. Separate studies of the peak current (i_p) and scan rate (v) reveal direct proportionality between i_p and v when the scan rates were varied between 10 and 80 mV/s, as expected for surface anchored species.[35,36] A summary of the peak potentials (E_{pa}, E_{pc}), formal potential [$E^{o'}$ = ($E_{pa}+E_{pc}$)/2], and E_{onset} for electrochemical reduction of PBZT and 2,6-PNBT is given in Table 1. The reduction potentials (i.e. $E^{o'}$) of the polymers are virtually identical (-1.86 V and -1.89 V vs. SCE).

Although the cyclic voltammogram (CV) for the reduction of PBZT has been reported previously[37], the peak potentials and formal potential found in the present study

are different from the previous report. In the earlier report[37], PBZT films were prepared on platinum electrodes from a very strong protonic acid (trifluoromethanesulfonic acid) and soaked overnight in water to eliminate the acid. The previously reported reduction CV on such a film showed two cathodic peak potentials at -1.70 and -1.92 V (vs. SCE) and two anodic peak potentials at -1.23 and -1.64 V. The peak with the more negative formal potential ($E^{o'}$ = -1.78 V) was speculated to be due to a defect or impurities. However, our results for PBZT show only one reduction wave with a corresponding formal potential of -1.86 V (vs. SCE) which is close to that previously assigned to the presence of impurities. It is likely that the trifluoromethanesulfonic acid was not completely removed in the previous study.[37] We have seen that films of PBZT prepared from methanesulfonic acid and rigorously washed and neutralized with 0.1M NaOH have identical CVs to that shown in Figure 7, i.e. have one reduction wave and identical formal reduction potential as for films prepared from nitromethane-$AlCl_3$.

Figures 8-10 present the reduction CVs of the remaining polybenzobisazoles of Chart I. As with PBZT and 2,6-PNBT, all the polymers exhibit only one reduction wave in their CVs and it is quasi-reversible. The corresponding reduction peak potentials, formal reduction potential ($E^{o'}$), and onset potential for reduction are summarized in Table 1. From a comparison of the reduction potentials of Figures 7-10 and Table 1 one sees a wide variation with molecular structure. One stricking feature of the results is that the formal reduction potential $E^{o'}$ and onset reduction potential E^{red}_{onset} vary by 0.6 V and 0.52 V, respectively, among the 8 polybenzobisazoles. The most difficult to reduce polymer in the set is PBO, the oxygen-containing polymer, with $E^{o'}$ of -2.18 V (vs. SCE). This means that the reduction potential of PBZT is higher than PBO's by 0.32 V which also implies that the reduced form of PBZT is thermodynamically more stable than that of PBO. On the

other hand, the most readily reduced polymers in the set of Chart I are PBTDV and PBTV which have essentially identical $E^{o'}$ values of -1.57 V and -1.60 V (vs. SCE) respectively. This is about 0.3 V higher than the formal reduction potential of PBZT.

A close examination of the CV results of Figures 7-10 and Table 1 reveals interesting effects of molecular structure on the reduction potentials. The large observed difference in the reduction $E^{o'}$ values of PBZT and PBO may seem surprising considering that oxygen is significantly more electronegative than sulfur (Pauling electronegativities of 3.5 and 2.5 respectively) and hence the *benzobisoxazole* ring should be more electron defficient than the *benzobisthiazole* ring. However, the more positive reduction potential of PBZT compared to PBO can be rationalized in terms of the better π-electron delocalization in PBZT which would allow efficient delocalization of the radical anion PBZT$^{-\cdot}$ compared to PBO$^{-\cdot}$. This explanation also holds for why the 4,4'-biphenylene-linked polymer, PBBZT, has an $E^{o'}$ value of -2.03 V (vs. SCE) which is 0.17 V lower than PBZT. The poorer electron delocalization in PBBZT compared to PBZT is a result of steric interactions of the ortho hydrogens of the 4,4'-biphenylene moiety. Thus, fusion of the two phenyl rings as in 2,6-naphthalene and 1,4-naphthalene moieties results in $E^{o'}$ values that are higher than in PBBZT. In fact, although the reduction potential of 2,6-PNBT is the same as that of PBZT, the reduction $E^{o'}$ of 1,4-PNBT is more positive than that of PBZT by 0.2 V. This last result can again be understood in terms of the better delocalization of the radical anion.

The *trans*-vinylene- and *trans,trans*-divinylene-linked polymers, PBTV and PBTDV, have the highest $E^{o'}$ values for reduction as a result of the good π-electron delocalization achieved in these polymers as evidenced by their electronic absorption spectra parameters (λ_{max}, E_g^{opt}; Table1). The reduction waves of these two polymers,

especially the cathodic peaks, are generally broad as seen in Figures 9 and 10. The origin of this broad feature of the CVs of PBTV and PBTDV is either because of a wider π^* band compared to PBZT and other polybenzobisazoles or it is morphological in nature. Our previous X-ray diffraction study of PBTDV indicated that this polymer has much closely packed chains than PBZT.[7a] Such a tight chain packing may affect the diffusion of the bulky counter cation ($n\text{-}C_4H_9)_4N^+$ in and out of the polymer during reduction.

The cyclic voltammetry results on electrochemical reduction of the series of polybenzobisazoles (Chart I) show that each of the polymers exhibits a quasi-reversible reduction in accord with the electron defficient nature of the *benzobisoxazole* and *benzobisthiazole* rings. The reduction potential ($E^{o'}$) of the series of polymers varies from -1.57 to -2.18 V (vs. SCE). Thus the relative ease of reduction is in the decreasing order: PBTDV, PBTV > 1,4-PNBT > PBTPV > PBZT, 2,6-PNBT > PBBZT > PBO. This order also represents the relative n-type dopability of the polymers into conducting polymers and the relative thermodynamic stability of the n-type doped material. We point out that it has previously been reported that PBZT can be electrochemically doped into an n-type conducting material with room temperature conductivity as high as 20 S/cm.[37] Our results suggest that all the 8 polybenzobisazoles can be n-type doped to conducting materials and furthermore that 4 of these polymers (PBTDV, PBTV, 1,4-PNBT and PBTPV) should be even superior to n-type doped PBZT. However, in terms of developing the polybenzobisazoles as efficient electron transporting materials for electrophotography, the reduction potential should be higher than that of molecular oxygen (~-0.8 V vs. SCE)[38] so that trapping of electrons by oxygen under ambient conditions is minimized. The highest reduction potential observed in these polymers ($E^{o'}$ = -1.57 V vs. SCE) is still significantly lower than that of molecular oxygen. Thus, although the present p-conjugated

polybenzobisazoles should in principle be electron transporting materials[39], this would only be in the absence of any traps for electrons such as molecular oxygen. One direction of future work on this class of polymers should be further modification of the polymers to achieve reduction potentials greater than -0.8 V(vs. SCE).

Electrochemical Oxidation. The electrochemical oxidation process in the polybenzobisazoles was not chemically reversible under the conditions of these experiments. Figure 11 shows representative CVs of the oxidation of PBTPV, 1,4-PNBT, and PBZT. Although the formal potential ($E^{o'}$) of the oxidation process cannot be obtained, the effect of molecular structure on oxidation can be inferred from the onset of oxidation (E^{ox}_{onset}) and the anodic peak potential (E_{pa}). The onset of electrochemical oxidation of PBTPV, 1,4-PNBT, and PBZT is at ~0.8, 0.85, and 1.1 V (vs. SCE) respectively; the corresponding anodic peak potential is at 1.31, 1.47, and 1.62 V respectively. A summary of the electrochemical oxidation parameters of all the polymers is given in Table 2. The data show that the onset of oxidation of the polybenzobisazoles varies between 0.75 to 1.3 V whereas the anodic peak potential varies between 0.85 to 1.72 V (vs. SCE).

The cyclic voltammetry results on electrochemical oxidation of the polybenzobisazoles show that the onset oxidation potential (E^{ox}_{onset}) and the peak oxidation potential (E_{pa}) are varied by 0.55 V and 0.87 V, respectively, by the variation in molecular structure. A qualitative ordering of the oxidation potential of the series of polymers is in the decreasing order: PBTDV < PBTPV, PBTV < 1,4-PNBT < PBZT, 2,6-PNBT < PBBZT, PBO. It is interesting that the same four polymers which had higher reduction potentials than PBZT also have lower oxidation potentials than PBZT. In fact, the relative ordering of the oxidation potentials of the 8 polymers is similar to the reversed

ordering of the reduction potentials. This means that the structural variation in Chart I affects the entire electronic structure of the polymers as will be discussed in more detail subsequently. The non-reversibility of the electrochemical oxidation of these polymers suggests that their one electron oxidized state (radical cation) is not stable and hence p-type dopability of the polymers to conducting materials is not going to be feasible. Thus, the polymers would also be poor hole transporting materials.

Electronic Structure. The measured electrochemical redox properties provide a basis for estimating and assesing the electronic structure of the π-conjugated polybenzobisazoles. To facilitate the discussion of the electronic structure of the polymers a schematic illustration of the relevant electronic energy levels and energy parameters is given in Figure 12. The electronic, optical, and optoelectronic properties of π-conjugated polymers have been theoretically and experimentally established to be dominated by the frontier orbitals, i.e. the highest occupied molecular orbital (HOMO or π level) and the lowest unoccupied molecular orbital (LUMO or π^* level).[40] The two energy parameters that establish the positions of these LUMO and HOMO levels relative to vacuum are electron affinity (EA) and ionization potential (IP) which are defined on the energy level diagram of Figure 12. The energy gap E_g is the separation between the HOMO and LUMO levels, hence $E_g = IP - EA$. Extensive prior studies of conjugated polymers have shown that the energy parameters EA and IP are related to the measured redox properties by[40]: $EA = E^{red}_{onset} + 4.4$ and $IP = E^{ox}_{onset} + 4.4$, where the onset redox potentials are in volts (vs. SCE) and EA and IP are in eV. The EA and IP values so obtained for the series of polybenzobisazoles are shown in Tables 1 and 2, respectively. The electrochemically determined energy gap ($E_g^{el} = IP - EA = E^{ox}_{onset} - E^{red}_{onset}$) is also given in Table 2.

The electron affinity values of the 8 series of polybenzobisthiazoles are in the range of 2.4 to 3.0 eV (Table 1), which reveals a 0.6 eV variation of EA with molecular structure. This means that there is a 0.6 eV difference between the LUMO levels of PBO which has the smallest electron affinity, and hence the highest lying LUMO, and the LUMO of PBTDV which has the largest electron affinity and also the lowest lying LUMO among the series of polymers. Comparing the electron affinities of PBO and PBZT, we see that the LUMO level of the sulfur-containing polymer (PBZT) is lowered by 0.3 eV relative to the oxygen-containing polymer. The LUMO levels of four of the polymers are within ±0.1 eV of that of PBZT. The electron affinity values of the polybenzobisazoles (2.4-3.0 eV) are to be compared to the EA values of other well known classes of π-conjugated polymers:[34,40] *trans*-polyacetylene (3.31 eV); polythiophene (2.96 eV); poly(*p*-phenylene) (2.58 eV); poly(*p*-phenylene vinylene) (2.71 eV); and poly(2,6-(4-phenyl quinoline)) (2.62 eV). Thus, some of the polybenzobisazoles have some of the largest known electron affinities among π-conjugated polymers.

The tabulated ionization potentials of the polybenzobisazoles are in the range of 5.2 eV for PBTDV, PBTV, and PBTPV to 5.7 for PBO and PBBZT. Thus, the variation in molecular structure seen in Chart I results in the observed 0.5 eV variation in the IP values and in the associated HOMO levels. Incorporation of *trans,trans*-vinylene, *trans*-vinylene or 1,4-phenylenebisvinylene in place of the *p*-phenylene moiety in the polybenzobisthiazoles results in an identical HOMO level which is 0.3 eV higher than that of PBZT. The effect of the heteroatoms (S, O) also shows up in the IP values, indicating that the HOMO of PBZT is shifted upwards relative to the HOMO of PBO by 0.2 eV. These ionization potentials of the polybenzobisazoles are also to be compared to those of other well known conjugated polymers:[34,40] *trans*-polyacetylene (4.73 eV); polythiophene

(5.2 eV); poly(*p*-phenylene) (5.42 eV); poly(*p*-phenylene vinylene) (5.11 eV); and poly(2,6-(4-phenyl quinoline)) (5.35 eV). Two of the polybenzobisazoles (PBO, PBBZT) have IP values that are much higher than the well-known conjugated polymers.[34,40] The other polymers in Table 2 have IP values that are comparable to the cited, previously studied, π-conjugated polymers[34,40] except *trans*-polyacetylene. Although the ionization potentials of some of the polymers (e.g. PBTDV, PBTV, and PBTPV) are sufficiently small to make oxidative (p-type) doping feasible,[1,34,40] our previous discussion of the irreversibility of the electrochemical oxidation process suggests that such p-type doped materials would be unstable.

The electrochemical energy gap E_g^{el} of the series of polymers varies from 2.20 to 3.27 eV (Table 2), indicating that this electronic structure parameter is tunable over about a 1 eV range. The energy gap determined from the optical absorption edge E_g^{opt} for the same polymers is in the range 2.07-2.76 eV, indicating that the tunability is only over about 0.7 eV. A comparison of E_g^{el} and E_g^{opt} shows that they are, within experimental errors, identical in three of the polymers (PBTDV, PBTV, and 1,4-PNBT) but that they differ by as much as 0.2 to 0.5 eV in the other polymers. Although the finding that E_g^{el} is not identical with E_g^{opt} may be explained in part by experimental uncertainties in the two different techniques, there is also a definitional or conceptual problem. The E_g^{opt} of conjugated polymers has commonly be taken as the optical absorption edge,[1,34,40] a view which assumes that the polymers are semiconductors and holds that the optical transitions are a result of band-edge-to-band-edge photoexcitations which produce free carriers. However, more and more evidence is pointing to the excitonic nature of the optical transitions in conjugated polymers[15b,22] in which case E_g^{opt} is best defined as the peak of the lowest energy HOMO-LUMO (π–π^*) transition. The energy of the lowest energy

absorption maximum in the optical spectra of the polybenzobisazoles is given in Table 1 and it deviates from the corresponding absorption edge by about 0.14 to 0.43 eV. Thus, taking E_g^{opt} to be the energy at the λ_{max} gives a better match with E_g^{el} of the series of polymers.

Refractive Index.

We have measured the wavelength dispersion of the isotropic refractive index $n(\lambda)$ of the conjugated rigid-rod polybenzobisazoles shown in Charts I and II to probe the effects of molecular structure on the linear optical properties of this class of materials which is of growing interest in photonics and nonlinear optics.[18,19] The measurement techniques and the details of the $n(\lambda)$ data analysis have previously been reported by our laboratory.[24] To interprete the measured refractive indices in terms of molecular structure we assume that the effects of molecular orientation and crystallinity are negligible. The polymer thin films (1.0-2.5 µm), prepared from isotropic solutions by spin coating, were optically transparent in the visible and excellent interference fringes could be obtained from them over a wide wavelength range and hence judged to be isotropic and largely amorphous. In contrast, semicrystalline and nonisotropic films were not optically transparent in the visible, were highly scattering, and interference fringes could not be obtained from them. Thus, we can examine the effects of molecular structure on refractive index of the series of polymers through two molecular parameters, i.e. polarizability (α) and molar volume (V) which appear in the Lorentz-Lorenz theoretical model[41] of the refractive index n:

$$\frac{n^2-1}{n^2+2} = \frac{4\pi N_A \alpha}{3V} \qquad (1)$$

where N_A is Avogadros number. The repeat unit molar volume V (cm^3/mol) of each polymer was calculated by the group contribution approach and is given in Table 3. E_g^{opt} shown in Table 1 was taken as an independent and approximate measure of the polarizability.[42]

Figures 13-16 show the refractive index dispersion $n(\lambda)$ of the series of polybenzobisazoles in Charts I and II. Each figure shows the comparative data for groups of the polymers. The solid lines through the data points in Figures 13-16 represent the fit of the $n(\lambda)$ data by the well-known Sellmeier dispersion equation. We have previously shown that the Sellmeier dispersion equation provides an excellent description of the $n(\lambda)$ data of many other conjugated polymers[24] and the results of Figures 13-16 similarly demonstrate an excellent fit. The refractive index $n(\lambda)$ data at selected wavelengths (λ= 1064, 1319, and 2500 nm) are shown in Table 3 along with the molar volume and Abbe number v_d'. The Abbe number reported here is that based on the three wavelengths indicated in Table 3 and it is a convenient numerical measure of the wavelength dispersion of the refractive index in the optically transparent and non-absorbing spectral region. One general observation on the refractive index data of Figures 13-16 and Table 3 is the highly dispersive nature of the refractive index of many of these polymers. In particular, the refractive indices of PBZI, PBZT, PBBZT, 1,4-PNBT, and 2,6-PNBT with Abbe numbers of 3.4-6.3 are the most dispersive. Although the Abbe numbers of some of the polybenzobisazoles (e.g. PBO, PBTDV, PBTPV, PBIPV, and BBB) are relatively higher (12-15), these are still fairly low compared to inorganic glasses, nonconjugated polymers, or conjugated polyimines (v_d' ~10-38).[24] Another general observation is the relatively large values of the refractive index of this series of polymers. For example, at 1064 nm the refractive index is between 1.74 and 2.03 among the different polymers whereas $n(\lambda = 2500$ nm) varies from 1.55 to 1.95.

Thus, off-resonance at 2500 nm, the refractive index varies by 0.40 among the series of polymers.

A comparison of the wavelength dispersion of the refractive index of the three 1,4-phenylene linked polymers PBZT, PBO, and PBZI which contain S, O, and NH heteroatoms, respectively, is shown in Figure 13. The dispesion of the $n(\lambda)$ data is similar in PBZT and PBZI which have Abbe numbers of 4.16 and 3.37, respectively. In contrast, the oxygen-containing polymer, PBO, with an Abbe number of 12.33 is much less dispersive. On the other hand, the off-resonance refractive index is identical in PBZT and PBO (1.70-1.71) whereas it is only 1.55 in PBZI. These results mainly reflect the combined effects of the heteroatoms on polarizability and molar volume. The similarity of the off-resonant refractive indices of PBZT and PBO arises from a balance between the greater polarizability (smaller E_g^{opt}) and larger molar volume of PBZT compared to PBO. However, a similar comparison between PBZI and PBZT shows that they both have similar polarizabilites (as measured by E_g^{opt}) and PBZI has a smaller molar volume (Table 3). On account of these two molecular factors alone one would expect PBZI to have a larger off-resonance refractive index which is contrary to the observation. An additional factor that may account for the 0.16 smaller refractive index of PBZI compared to PBZT is the electron density contribution to polarizability not accounted for by E_g^{opt}. Another factor still is the known moisture absorption of PBZI (up to 9 wt%)[43] which could significantly increase the molar volume above the value shown in Table 3 for the pure polymer; in contrast, PBZT, PBO, and their derivatives do not absorb any moisture.

The refractive index dispersion data for the three new polybenzobisazoles (PBBZT, 2,6-PNBT, and 1,4-PNBT) are shown in Figure 14. The optical dispersion as measured by the Abbe number (5.00-6.31) is very similar in all three polymers. Although the off-

resonant refractive indices of all three materials at 2500 nm is fairly close 1.75-1.81, the small difference (<3%) and subtle differences between them could not be accounted for by consideration of the molar volume and E_g^{opt} alone. This means that the polarizability must include the effects of electron density variation in addition to electron delocalization (E_g^{opt}).

The wavelength dispersion of the refractive index of PBTPV, PBTDV, and PBIPV are shown in Figure 15. The optical dispersion in these three polymers, represented by Abbe numbers of 12.38-15.20, is the least among the series of polymers investigated (Charts I and II). A comparison between the S-containing PBTPV and NH-containing PBIPV, which are otherwise structurally similar, shows a large difference of 0.22 in their off-resonant refractive indices at 2500 nm (1.95 versus 1.73). Although PBTPV has a slightly higher molar volume and E_g^{opt} than PBIPV, its higher electron density more than compensates and thus results in a net increase of refractive index. The 0.08 (or 4%) smaller $n(\lambda = 2500$ nm) of PBTDV compared PBTPV can be similarly explained by the greater electron density of PBTPV which translates into a large polarizability. A further insight into the difference between the $n(\lambda)$ data of this two latter polymers comes from the recently established molar refraction of functional groups found in π-conjugated polymers.[44] The *trans,trans*-divinylene moiety in PBTDV has a molar refraction, and hence polarizability, that is 32% less than the molar refraction and polarizability of 1,4-phenylenebisvinylene moiety in PBTPV.[44]

The effect of the ladder and semi-ladder structures on the refractive index of polybenzobisimidazobenzophenanthrolines (BBL, BBB) was also investigated. Figure 16 shows the $n(\lambda)$ data for BBL and BBB films. The ladder polymer BBL has a slightly more dispersive refractive index than the semi-ladder BBB (v_d' of 8.45 and 12.43, respectively). BBL also has a slightly larger refractive index at 2500 nm (1.88) compared to BBB (1.84).

The observed difference in the refractive index data of BBL and BBB are readily accounted for by the larger polarizability (e.g. smaller E_g^{opt}, 1.78 versus 1.82 eV) and smaller molar volume of BBL.

CONCLUSIONS

This study has examined the effects of molecular structure on the redox properties, the electronic structure parameters, and the refractive index of conjugated polybenzobisazoles. It was found that the one-electron electrochemical reduction of the series of polymers in Chart I was reversible which implies that the materials can be reductively (n-type) doped to conducting polymers and also function as electron transporting materials in the absence of oxygen. The reduction potential ($E^{o'}$) varied from -1.57 to -2.18 V (vs SCE). In contrast, the one-electron electrochemical oxidation of the polymers was not reversible which indicates that oxidative (p-type) doping to conducting polymers was not feasible. The electron affinity and ionization potential, estimated from the redox properties, were 2.4 to 3.0 and 5.2 to 5.7 eV, respectively, and are useful for establishing the relative LUMO and HOMO levels in the materials and for rationalizing their electronic and photophysical properties.

The wavelength dependent refractive index of the polybenzobisazoles was found to vary with the backbone structure and heteroatom, by as much as 0.4 at 2500 nm. The off-resonant refractive index at 2500 nm was quite large (1.55-1.95). The NH-containing polybenzobisimidazoles have significantly lower refractive indices compared to their corresponding sulfur- and oxygen-containing polybenzobisazoles. The potential application of these polymers in integrated optics and nonlinear optical devices was recently explored with a demonstration of channel waveguides fabricated from PBZT[23,45] and 1,4-PNBT.[45]

ACKNOWLEDGEMENTS

R E F E R E N C E S

1. Brédas, J. L.; Chance, R. R., Eds. *Conjugated Polymeric Materials: Opportunity in Electronics, Optoelectronics, and Molecular Electronics*; Kluwer Academic Publishers: Dordrecht, Holand, 1990.

2. Burroughes, J. H; Bradley, D. D. C.; Brown, A. R.; Marks, R. N.; Mackay, K.; Friend, R. H.; Burn, P. L.; Holmes, A. B. *Nature* **1990**, *347*, 539-541.

3. Marder, S. R.; Sohn, J. E.; Stucky, G. D., Eds. *Materials for Nonlinear Optics: Chemical Perstectives*; American Chemical Society: Washington, DC, 1991.

4. Jenekhe, S. A., Ed. *Macromolecular Host-Guest Complexes: Optical, Optoelectronic, and Photorefractive Properties and Applications;* Materials Research Society: Pittsburgh, 1992.

5. (a) Miller, J. S. *Adv. Mater.* **1993**, *5*, 587-. (b) Miller, J. S. *Adv. Mater.* **1993**, *5*, 671.

6. Stegeman, G. I.; Miller, A. in *Photonics in Switching*, vol. 1, Midwinter, J. E., Editor, Academic Press: London, 1993.

7   (a) Osaheni, J. A.; Jenekhe, S. A. *Chem. Mater.* **1992**, *4*, 1282-1290.

    (b) Osaheni, J. A.; Jenekhe, S. A. *Macromolecules* **1993**, *26*, 4726-4728.

8. (a) Agrawal A. K.; Jenekhe, S. A. *Macromolecules* **1993**, *26*, 895-905. (b) Agrawal A. K.; Jenekhe, S. A. *Chem. Mater.* **1993**, *6*, 633-640. (c) Agrawal A. K.; Jenekhe, S. A. *Macromolecules.* **1991**, *24*, 6806-6808.

9. Chen, W. C.; Jenekhe, S. A. *Macromolecules* **1992**, *25*, 5828-5835.

10. Yang, C. J.; Jenekhe, S. A. *Chem. Mater.* **1991**, *3*, 878-887.

11. Agrawal, A. K.; Jenekhe, S. A. *Chem. Mater.* **1992**, *4*, 95-104.

12. Jenekhe, S. A.; Johnson, P. O.; Agrawal, A. K. *Macromolecules* **1989**, *22*, 3216-3222. (b) Jenekhe, S. A.; Johnson, P. O. *Macromolecules* **1990**, *23*, 4419-4429.

13. Abkowitz, M. A.; Stolka, M.; Antoniadis, H.; Agrawal, A. K.; Jenekhe, S. A. *Solid State Commun.* **1992**, *83*, 937-941.

14. Antoniadis, H.; Abkowitz, M. A.; Osaheni, J. A.; Jenekhe, S. A.; Stolka, M. *Synthetic Metals* **1993**, *60*, 149-157.

15. (a) Osaheni, J. A.; Jenekhe, S. A.; Perlstein, J. *Appl. Phys. Lett.* **1994**, *64*, 3112-3114. (b) Osaheni, J. A.; Jenekhe, S. A.; Perlstein, J. *J. Phys. Chem.* **1994**, *98*, 12727-12736.

16. Osaheni, J. A.; Jenekhe, S. A.; Vanherzeele, H; Meth, J. S. Sun, Y.; MacDiarmid, A. G. *J. Phys. Chem.***1992**, *96*, 2830-2836.

17. (a) Agrawal A. K.; Jenekhe, S. A. Vanherzeele, H.; Meth, J. S. *J. Phys. Chem.* **1992**, *96*, 2837-2843.

18. Vanherzeele, H.; Meth, J. S.; Jenekhe, S. A.; Roberts, M. F. *J. Opt. Soc. Am. B* **1992**, *9*, 524-532.

19. Jenekhe, S. A.; Osaheni, J. A.; Vanherzeele, H.; Meth, J. S. *Chem. Mater.* **1992**, *4* , 683-687.

20. (a) Jenekhe, S. A.; Yang, C. J.; Vanherzeele, H.; Meth, J. S. *Chem. Mater.* **1991**, *3*, 985-987. (b) Yang, C. J.; Jenekhe, S. A.; Vanherzeele, H.; Meth, J. S. *Mater. Res. Soc. Proc* . **1992**, *247*, 247-252.

21. Osaheni, J. A.; Jenekhe, S. A. *Macromolecules* **1994**, *27*, 739-742.

22. Jenekhe, S. A.; Osaheni, J. A. *Science* **1994**, *265*, 765-768.

23. Mittler-Neher, S.; Otomo, A.; Stegeman, G. I.; Lee, C. Y.-C.; Mehta, R.; Agrawal, A. K.; Jenekhe, S. A. *Appl. Phys. Lett.* **1993**, *62*, 115-117.

24. Yang, C. J.; Jenekhe, S. A. *Chem. Mater.* **1994**, *6*, 196-203.

25. Seferis, J. C. in *Poymer Handbook*; Brandrup, J.; Immergut, E., Eds. Wiley: New York, 1989; pp VI 451-461.

26. Van Krevelen, D. W. *In Computational Modeling of Polymers*, Bicerano, J., Ed., Marcel Dekker: New York, 1992; pp 55-123.

27. Wolfe, J. F.; Arnold, F. E. *Macromolecules* **1981**, *14*, 909-915. (b) Wolfe, J. F.; Loo, B. H.; Arnold, F. E. *Macromolecules* **1981**, *14*, 915-920.

28. (a) Wolfe, J. F. in *Encylopaedia of polymer Science and Engineering*, Wiley: New York, 1988; vol. 11, pp 601-635. (b) Stuez, D. E.; Serad, G. A. In *Encylopaedia of polymer Science and Engineering*, Wiley: New York, 1988; vol. 11, pp 572-601.

29. (a) Dang, T. D.; Tan, L. S.; Wei, K. H.; Chuah, H. H.; Arnold, F. E. *Polym. Mater. Sci. Eng.* **1989**, *60*, 424-425. (b) Tan, L. S.; Reinhardt, B. A.; Soloski, E. J.; Simko, S. R.; Dillard, A. G. *Polym. Prepr. (Am. Chem, Soc., Div. Polym. Chem.)* **1992**, *33(1)*, 1062-1063.

30. Roberts, M. F.; Jenekhe, S. A. *Polym. Commun.* **1990**, *31*, 215-217.

31. Osaheni, J. A.; Jenekhe, S. A. *J. Am. Chem. Soc.*, submitted.

32. Swanepoel, R. *J. Opt. Soc. Am.* **1985**, *A2*, 1339-1343.

33. Shen, D. Y.; Hsu, S. L. *Polymer* **1982**, *23*, 969-973.

34. Agrawal, A. K.; Jenekhe, S. A. *J. Phys. Chem.*, submitted.

35. (a) Diaz, A. F.; Bargon, J. In *Handbook of Conducting Polymers*; Skotheim, T. A. Ed.; Marcel Dekker: New York, 1986; Vol. 1, Chapter 3. (b) Tourillon, G. *ibid.* Chapter 5. (c) MacDiarmid, A. G.; Kaner, R. B. *ibid.* Chapter 20.

36. Murray, R. W. In *Electroanalytical Chemistry*; Bard, A. J., Ed.; Marcel Dekker: New York; Vol. 13, pp191-368. (b) Peerce, P. J.; Bard, A. J. *J. Electroanal. Chem.* **1980**, *114*, 89-115.

37. Depra, P. A.; Gaudiello, J. G.; Marks, T. J. *Macromolecules* **1988**, *21*, 2295-2297.

38. Weast, R. C. Ed. *CRC Handbook of Chemistry and Physics*, 68th ed.; CRC Press Inc.: Boca Raton, Florida, 1987.

39. Abkowitz, M. A.; Stolka, M. A. In *Polymers for Advanced Technologies,* Lewin, M., Ed.; VCH Publishers: Weinheim, Germany, 1990; pp 225-260.

40. (a) Bredas, J. L.; Silbey, R.; Boudreaux, D. S.; Chance, R. R. *J. Am. Chem. Soc.* **1983**, *105*, 6555-6559 (b) Eckhardt, H.; Jen, K. Y.; Shacklette, L. W.; Lefrant, S. In ref. 1 pp.305-320. (c) Bredas, J. L.; Chance, R. R.; Baughman, R. H.; Silbey, R. *J. Chem. Phys.* **1982**, *76*, 3673-.

41. Lorentz, H. A. *Ann. Phys.* **1880**, *9*, 641. (b) Lorenz, L. V. *Ann. Phys.* **1880**, *11*, 70.

42. Flytzanis, C. In *Nonlinear Optical Properties of Organic Molecules and Crystals*, Vol. 2, Chemla, D. S.; Zyss, J., Eds., Academic Press: New York, 1987; pp121-

135.

43. Osaheni, J. A.; Jenekhe, S. A. *Macromolecules*, **1995**, *28*, in press.

44. Yang, C. J.; Jenekhe, S. A. *Chem. Mater.,* submitted.

45. Ihlein, G.; Menges, B.; Mittler-Neher, S.; Osaheni, J. A.; Jenekhe, S. A. *Nonlinear Optics*, in press.

Table 1. Summary of the optical absorption and electrochemical reduction of thin films of polybenzobisazoles.

Polymer	Optical Absorption		Electrochemical Reduction[a]				
	λ_{max} (nm)	$\pi-\pi^*$ gap E_g^{opt}, (eV)	E_{pc} (V)	E_{pa} (V)	$E^{o'}$ (V)	E_{onset}^{red} (V)	EA (eV)
PBBZT	415 (2.99)[b]	2.61	-2.22	-1.84	-2.03	-1.80	2.6
2,6-PNBT	435 (2.85)	2.48	-2.16	-1.63	-1.89	-1.75	2.7
1,4-PNBT	435 (2.85)	2.36	-1.76	-1.56	-1.66	-1.60	2.8
PBZT	438, 468 (2.65)	2.48	-2.03	-1.69	-1.86	-1.75	2.7
PBTPV	475 (2.61)	2.25	-1.91	-1.62	-1.77	-1.68	2.7
PBTV	470 (2.64)	2.21	-1.80	-1.39	-1.60	-1.46	2.9
PBTDV	500 (2.48)	2.07	-1.75	-1.38	-1.57	-1.45	3.0
PBO	401, 427 (2.90)	2.76	-2.38	-1.97	-2.18	-1.97	2.4

a. E_{pc} = Cathodic peak potential; E_{pa} = Anodic peak potential; E_{onset}^{red} = Onset of reduction; EA = electron affinity. b. λ_{max} in eV.

Table 2. Summary of electrochemical oxidation[a] and energy gap of thin films of polybenzobisazoles.

Polymer	E_{pa} (V)	E_{pc} (V)	E^{ox}_{onset} (V)	IP (eV)	E_g^{el} (eV)
PBBZT	1.72	b	1.30	5.7	3.10
2,6-PNBT	1.60	b	1.1	5.5	2.85
1,4-PNBT	1.47	b	0.85	5.3	2.36
PBZT	1.62	b	1.1	5.5	2.85
PBTPV	1.31	b	0.80	5.2	2.48
PBTV	1.35	b	0.80	5.2	2.26
PBTDV	0.85	b	0.75	5.2	2.20
PBO	1.70	b	1.30	5.7	3.27

a. E_{pa} = Anodic peak potential; E^{ox}_{onset} = Onset of oxidation; IP = ionization potential; E_g^{el} = electrochemical gap.
b. The oxidation process is not reversible.

Table 3. Molar Volume, Refractive Index of thin films at selected Wavelengths, and Abbe number[a] of Polybenzobisazoles.

Polymer	Molar Volume (cm^3/mol)	n_{1064}	n_{1319}	n_{2500}	v_d'
PBZT	195	1.89	1.79	1.70	4.16
PBO	165	1.77	1.74	1.71	12.33
PBZI	185	1.74	1.64	1.55	3.37
PBBZT	270	1.99	1.90	1.81	5.00
1,4-PNBT	243	1.88	1.82	1.75	6.31
2,6-PNBT	243	1.97	1.88	1.80	5.18
PBTDV	184	1.93	1.90	1.87	15.00
PBTPV	249	2.03	1.99	1.95	12.38
PBIPV	239	1.78	1.76	1.73	15.20
BBL	-	1.99	1.93	1.88	8.45
BBB	-	1.91	1.87	1.84	12.43

a. Abbe number $v_d' = (n_{1319}-1)/(n_{1064}-n_{2500})$.

FIGURE CAPTIONS

Figure 1. ^{1}H NMR Spectrum of PBBZT in $CD_3NO_2/AlCl_3$ and its assignment.

Figure 2. ^{1}H NMR Spectrum of 1,4-PNBT in $CD_3NO_2/AlCl_3$ and its assignment.

Figure 3. FTIR absorption spectra of (a) PBZT, (b) PBBZT, (c) 1,4-PNBT, and (d) 2,6-PNBT.

Figure 4. TGA Thermograms of (a) PBBZT and (b) 2,6-PNBT heated in nitrogen atmosphere.

Figure 5. Optical absorption spectra of thin films of (1) PBZT, (2) PBBZT, (3) 2,6-PNBT, and (4) 1,4-PNBT.

Figure 6. Solution optical absorption spectra of (1) PBBZT, (2) 2,6-PNBT, and (3) 1,4-PNBT in methanesulfonic acid (at $\sim$5x10^{-6}M).

Figure 7. Cyclic Voltammogram of the reduction of (a) PBZT and (b) 2,6-PNBT in 0.1M TBABF4 /acetonitrile at a scan rate of 20 mV/s.

Figure 8. Cyclic Voltammogram of the reduction of (a) 1,4-PNBT and (b) PBBZT in 0.1M TBABF4 /acetonitrile at a scan rate of 20 mV/s.

Figure 9. Cyclic Voltammogram of the reduction of (a) PBTDV and (b) PBTPV in 0.1M TBABF4 /acetonitrile at a scan rate of 20 mV/s.

Figure 10. Cyclic Voltammogram of the reduction of (a) PBTV, (b) PBZT, and (c) PBO in 0.1M TBABF4/acetonitrile at a scan rate of 20 mV/s.

Figure 11. Cyclic Voltammogram of the oxidation of (a) PBTPV, (b) 1,4-PNBT, and (c) PBZT in 0.1M TBABF4 /acetonitrile at a scan rate of 20 mV/s.

Figure 12. A schematic illustration of the electronic structure parameters.

Figure 13. Wavelength dispersion of the refractive indices of (1) PBZT, (2) PBO, and (3) PBZI and their Sellmeier equation fit.

Figure 14. Wavelength dispersion of the refractive indices of (1) PBBZT, (2) 2,6-PNBT, and (3) 1,4-PNBT and their Sellmeier equation fit.

Figure 15. Wavelength dispersion of the refractive indices of (1) PBTPV, (2) PBTDV, and (3) PBIPV and their Sellmeier equation fit.

Figure 16. Wavelength dispersion of the refractive indices of (1) BBL and (2) BBB and their Sellmeier equation fit.

Chart I
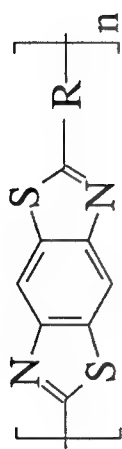
1

R
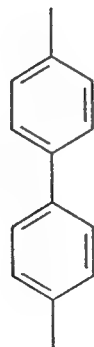
a. (PBBZT)
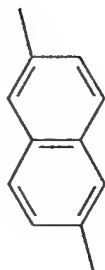
b. (2,6-PNBT)
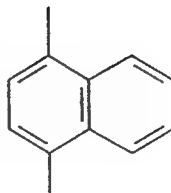
c. (1,4-PNBT)
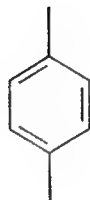
d. (PBZT)
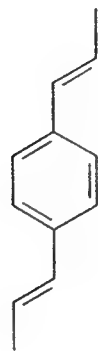
e. (PBTPV)
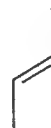
f. (PBTV)

g. (PBTDV)

2. PBO

Chart II

PBZI

PBIPV

BBL

BBB

figure 1.

Chemical Shift δ (ppm)

Figure 2
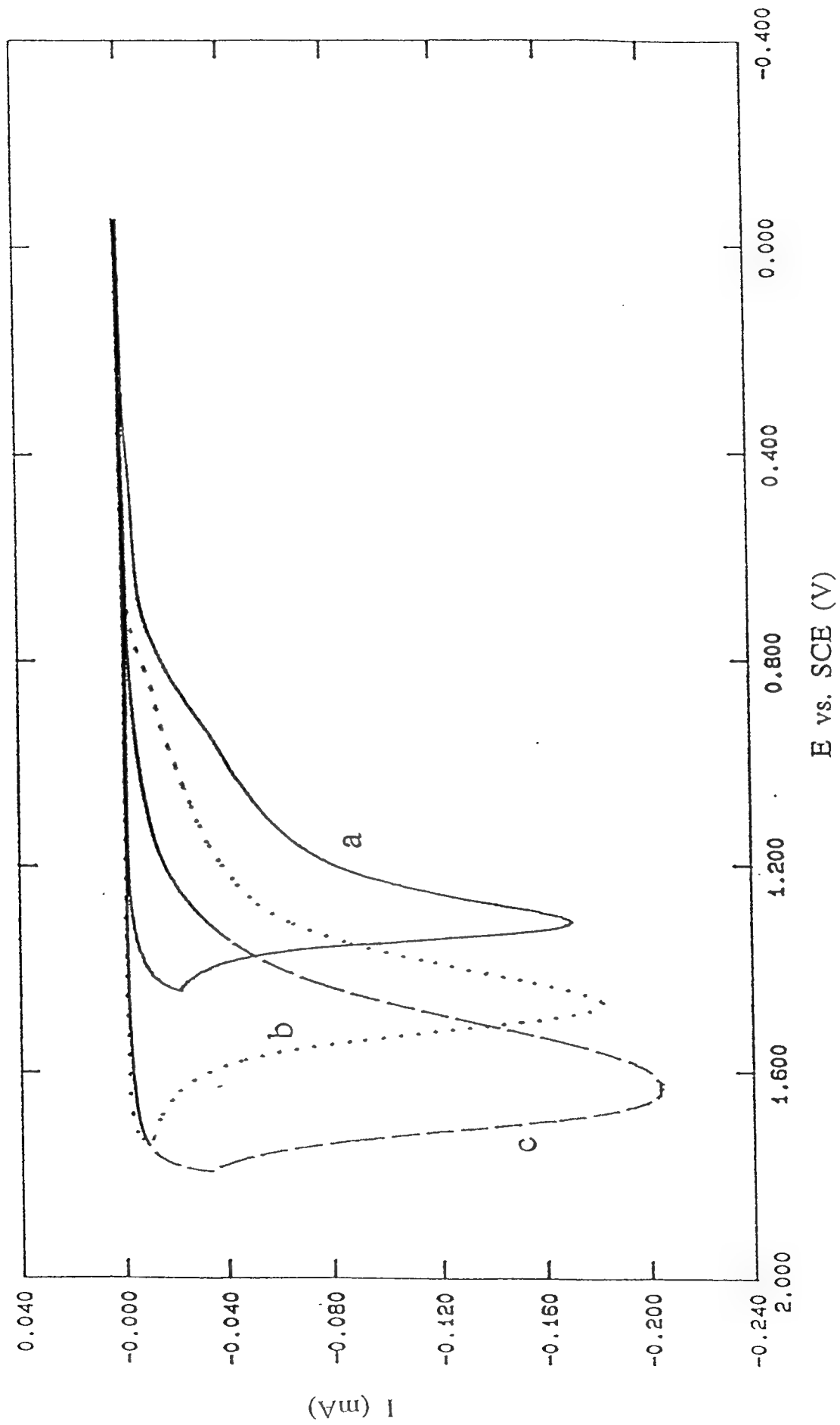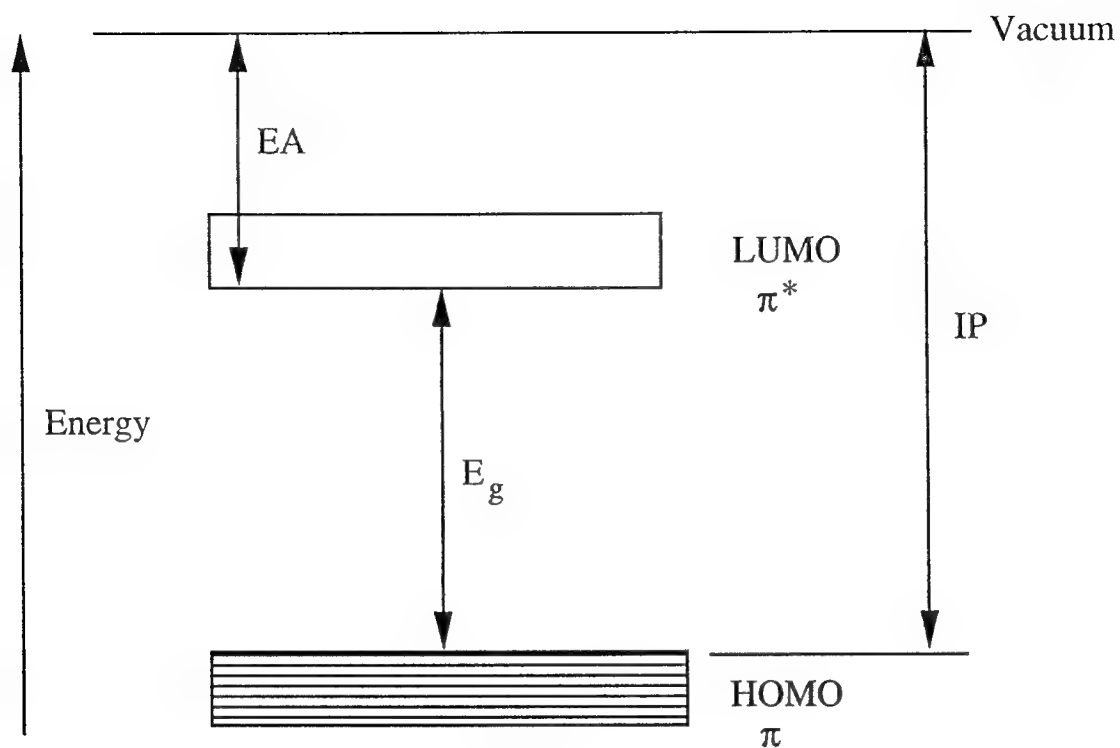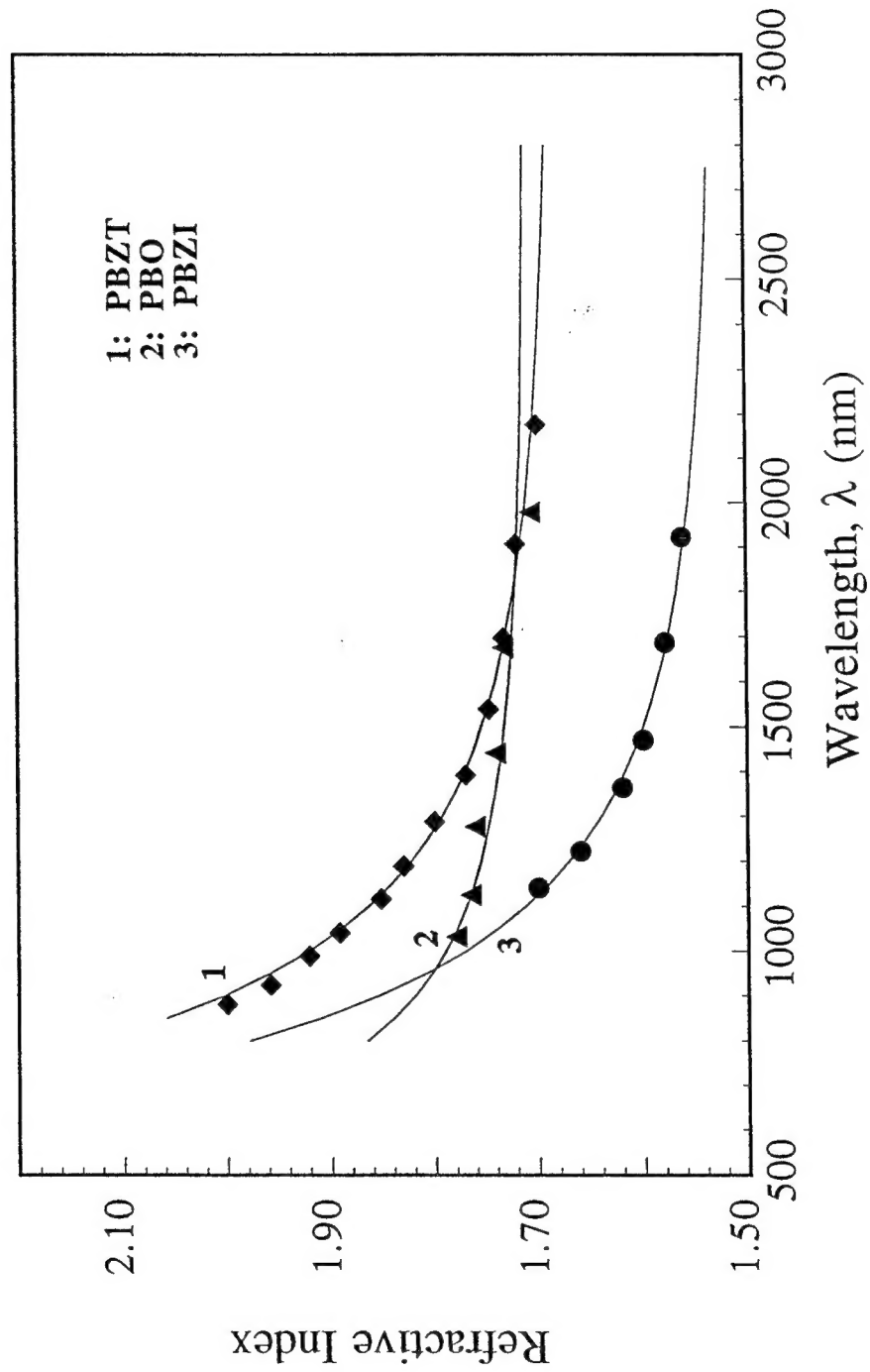
Chemical Shift δ (ppm)

Figure 3

Wavenumber (cm^{-1})

Fig. 4
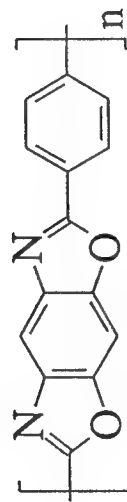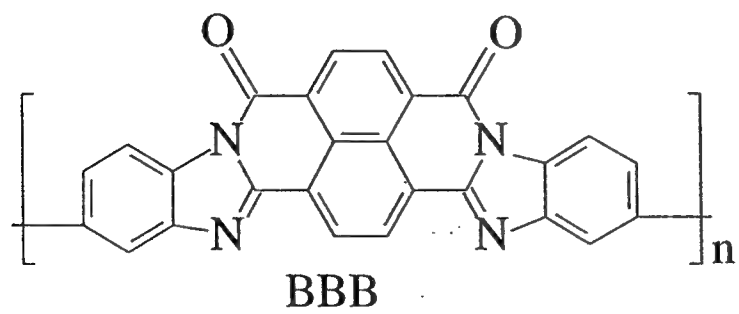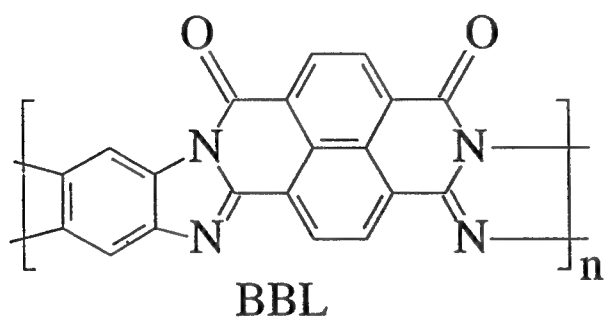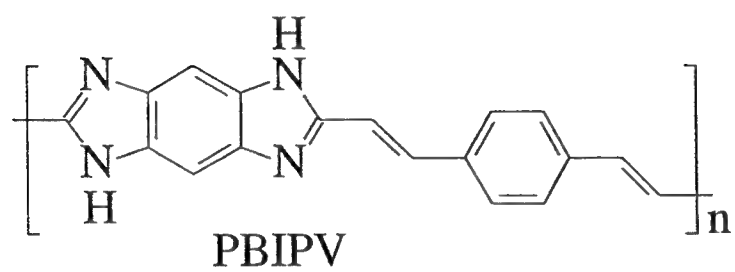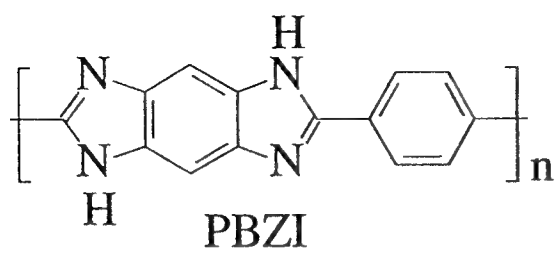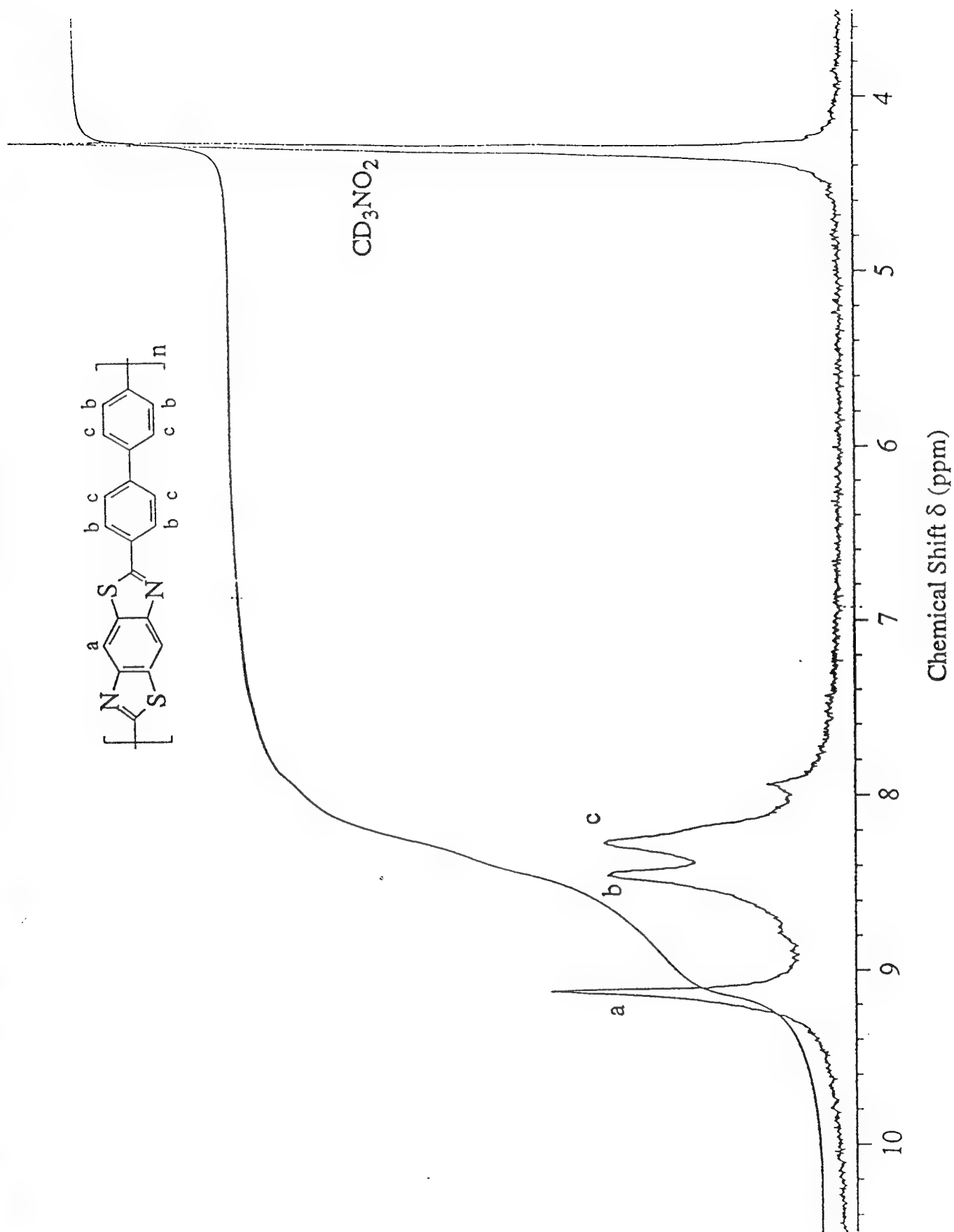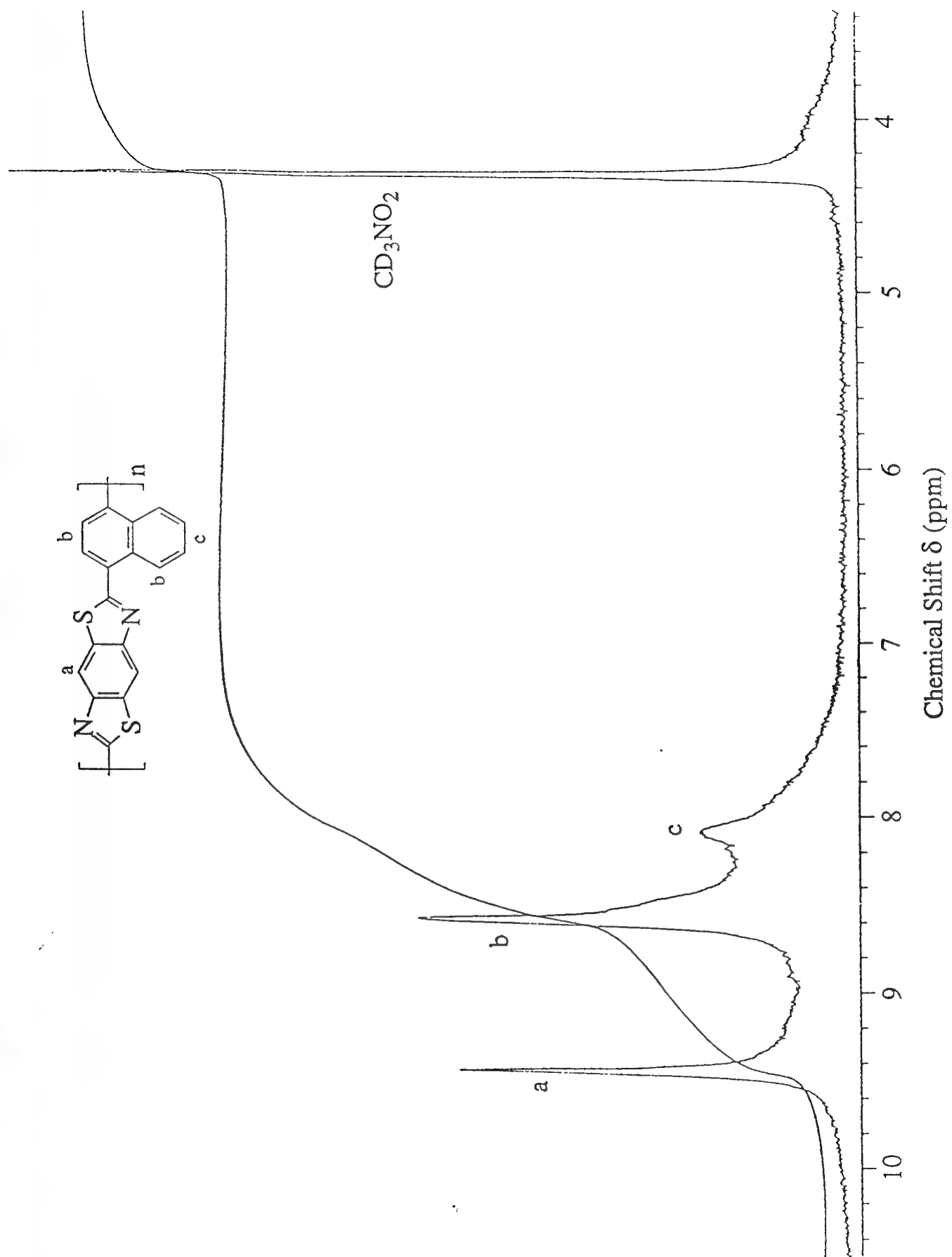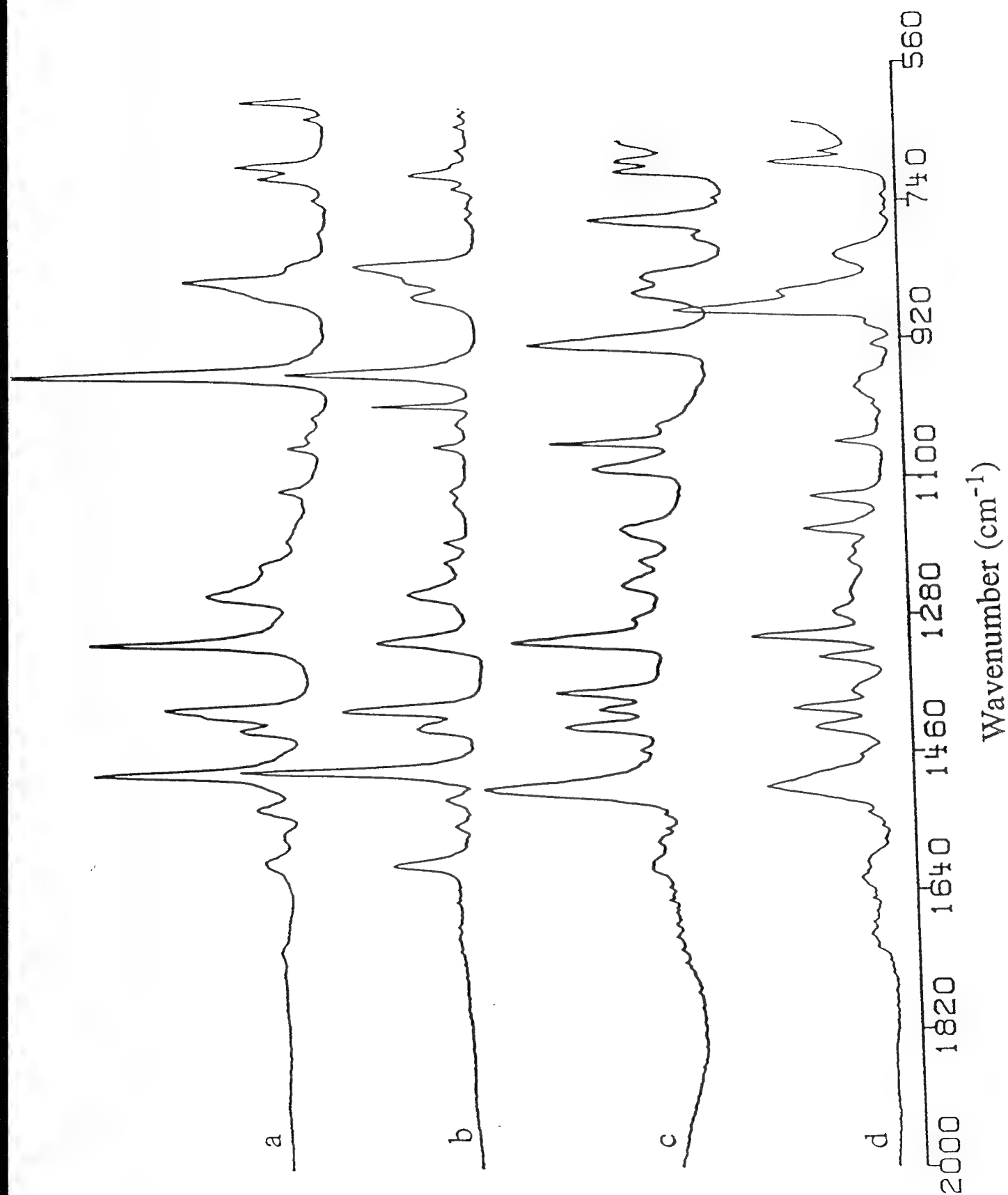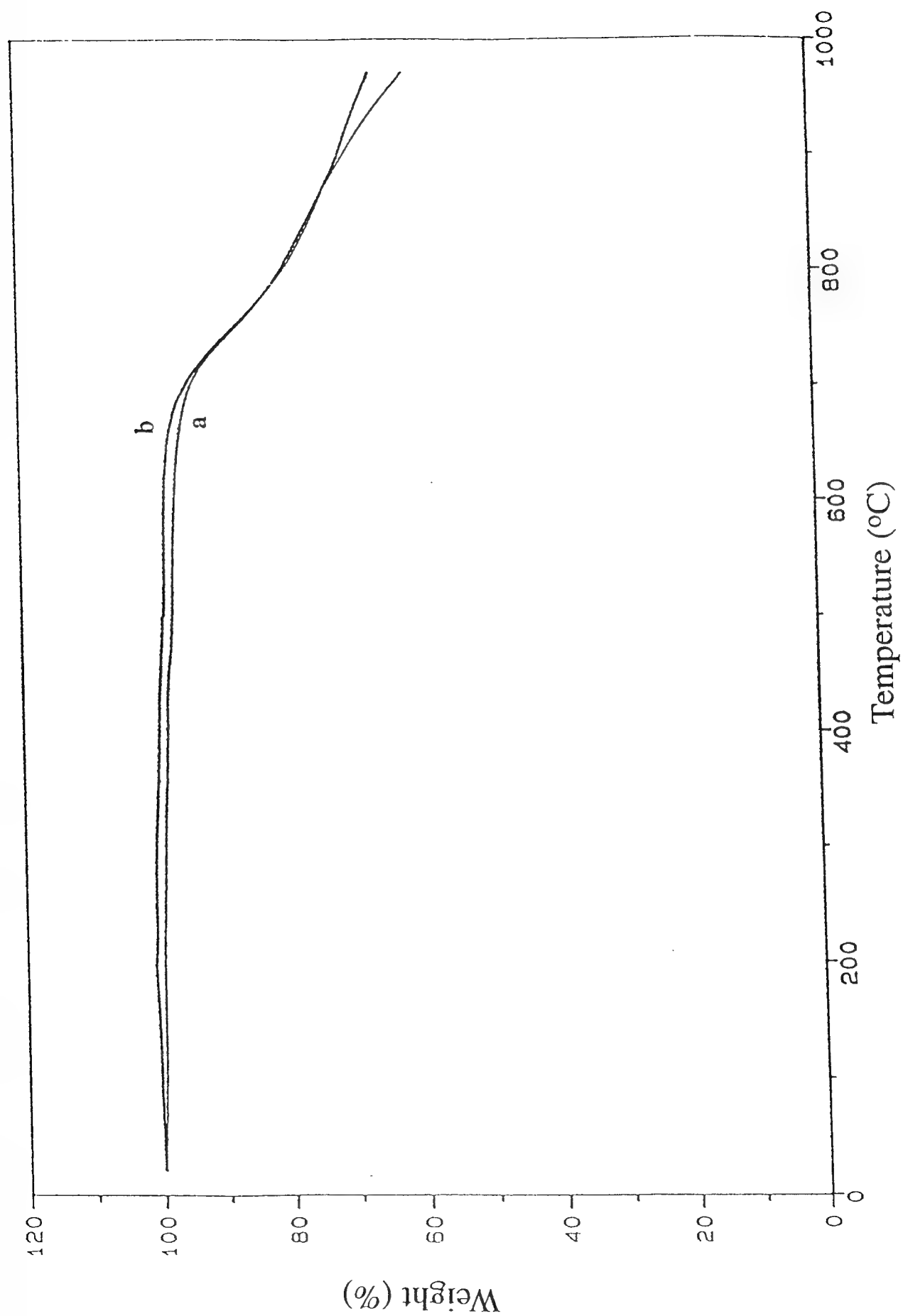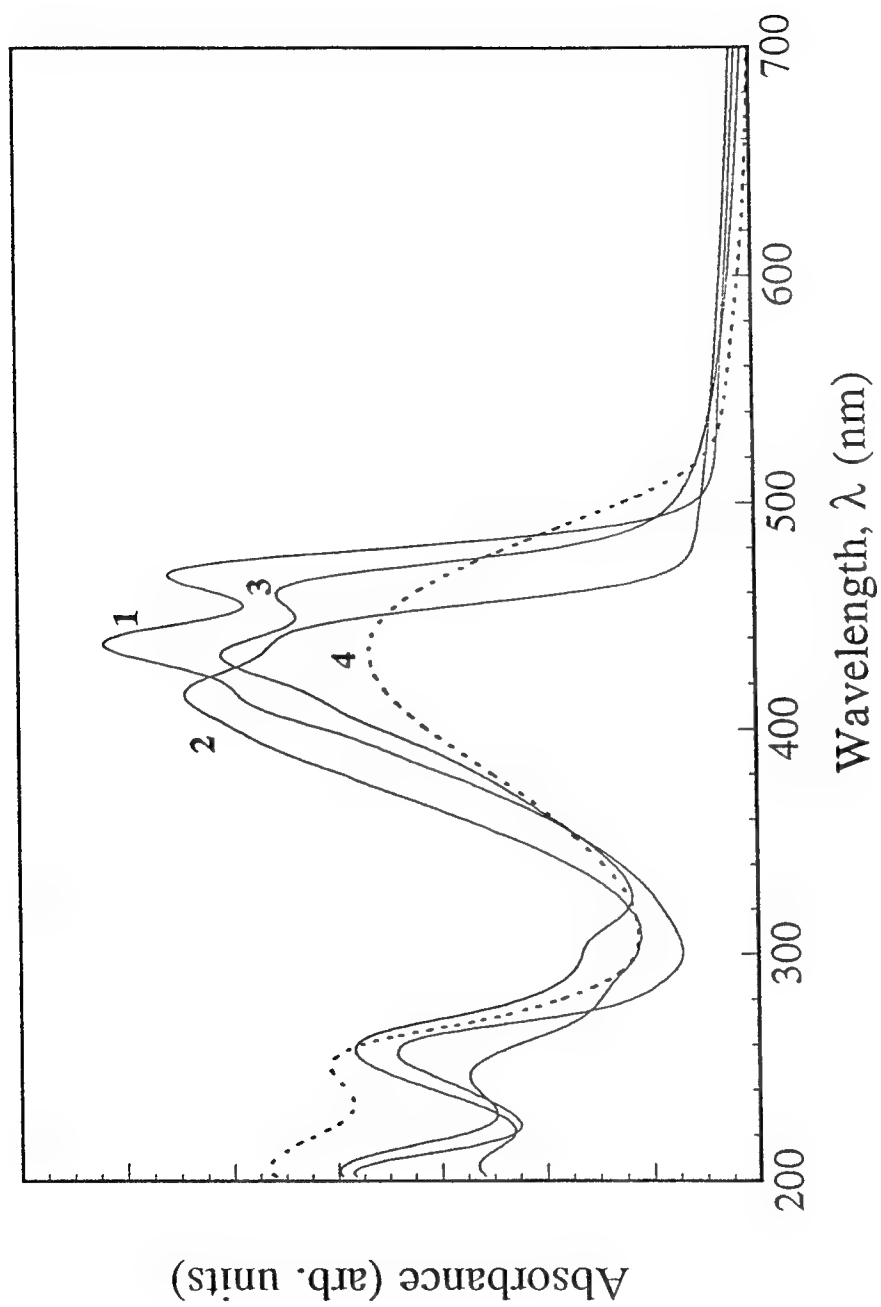
Figure 5

Figure 6

Figure 7.

Figure 8

Figure 9

Figure 10.

Figure 11

I (mA)

E vs. SCE (V)

Figure 12

Figure 13

Refractive Index vs. Wavelength, λ (nm)

1: PBZT
2: PBO
3: PBZI

Figure 14

Figure 15

Figure 16